Monolithically Integrated Resonator Microoptic Gyro on Silica Planar Lightwave Circuit

Kenya Suzuki, Koichi Takiguchi, *Member, IEEE*, and Kazuo Hotate, *Senior Member, IEEE*

***Abstract*—In this paper, we report a novel configuration of resonator microoptic gyro (MOG), which is monolithically integrated on silica planar lightwave circuit (PLC) with countermeasures for noise factors. Optical ring-resonator gyros suffer mainly from polarization fluctuation induced noise and backscattering induced noise. We discuss eigenstate of polarization in the waveguide to clarify behavior of the former and propose a countermeasure with control of the waveguide birefringence. As for the latter, binary phase shift keying (B-PSK) with a special signal processing is proposed. Thermooptic (TO) phase modulation is the only one scheme to apply B-PSK in the silica waveguide, whose bandwidth is limited to ~1 KHz. To utilize the narrow bandwidth of the TO modulator effectively, we propose an electrical signal processing scheme and a modulation waveform to compensate the frequency response. By constructing an experimental setup, suppression of the backscattering induced noise is demonstrated, and the gyro output is observed with applying an equivalent rotation.**

***Index Terms*—Binary phase shift keying (B-PSK), eigenstate of polarization (ESOP), gyroscopes, integrated optics, interference suppression, optical passive ring-resonator gyro, planar lightwave circuit (PLC).**

I. Introduction

OPTICAL gyro are indispensable devices for navigation systems, which require preciseness in rotation measurement. Though fiber-optic gyros (FOG's) [1]–[3] have shown good performance, they are relatively expensive due to complexity in fabrication process and a large number of the components. Therefore it is not easy to apply FOG's to consumer needs, such as car navigation, robotics and so on. In other words, there is a requirement for a cheap and compact optical gyro. To realize the needs, considerations have been done about integrated optical gyro by microoptics or optical waveguides [4]–[6]. However, configurations proposed previously have not had suitable countermeasure for the noise factors, such as backscattering induced noise or polarization fluctuation induced noise in resonator type [4], [5], or temperature fluctuation error in interferometer type [6].

On the other hand, silica planar lightwave circuits (PLC's) are promising devices, not only for optical communication, but also for optical precise measurement. Actually, several optical integrated sensors are investigated using the silica waveguide, for example, displacement sensor [7], [8], pressure sensor [9], accelerometer [10], current sensor [11], and so on. These optical integrated sensors have advantages, such as compactness, stability, reliability, easiness in fabrication.

In this paper, we describe the feasibility of resonator microoptic gyro (MOG) integrated on the silica planar lightwave circuit. First, we propose a novel configuration of resonator MOG with countermeasures both for the backscattering induced noise and polarization fluctuation induced noise, and then show the performance of the countermeasures. Finally, we demonstrate the function as a gyro.

Manuscript received March 10, 1999; revised September 15, 1999.

K. Suzuki and K. Hotate are with the Department of Electronic Engineering, School of Engineering, The University of Tokyo, Tokyo 113-8656, Japan.

K. Takiguchi is with the NTT Photonics Laboratories, Ibaraki 319-1193, Japan.

Publisher Item Identifier S 0733-8724(00)01467-5.

II. Resonator Microoptic Gyro on Silica Planar Lightwave Circuit and its Noise Factors

A. Proposed Configuration of Microoptic Gyro with Countermeasures for Noise Factors

Ring resonator configuration [12] might be suitable for microoptic gyro, in order to minimize the gyro system and to use cheaper semiconductor laser rather than broad-band light source such as superluminescent laser diode (SLD). For the resonator, low loss waveguide is necessary to obtain a high finesse. In other words, the loss of the waveguide determines the sensitivity of the MOG. Because of the above reasons, we adopt low loss silica PLC as the waveguide with following configuration.

Fig. 1 shows our configuration of MOG. It has a thermooptic phase modulator, a Mach–Zehnder interferometric switch and pressure applying amorphous silicon film on a silica waveguide as countermeasures for noise factors. Details will be discussed below.

B. Theoretical Limitation of Sensitivity and Fundamental Characteristics of Fabricated PLC for MOG

Resonance curve of a ring resonator is given by

$$R(\beta L)=\gamma_c^2\left(1-\frac{\kappa(1-\gamma^2)}{(1-\sqrt{1-\kappa}\gamma)^2+4\sqrt{1-\kappa}\gamma\sin^2\dfrac{\beta L}{2}}\right) \tag{1}$$

$$\gamma=\gamma_c\gamma_w \tag{2}$$

where

- κ coupling ratio of directional coupler;
- γ_c amplitude transmissivity of the coupler;
- γ_w amplitude transmissivity of the waveguide;
- β propagation constant;

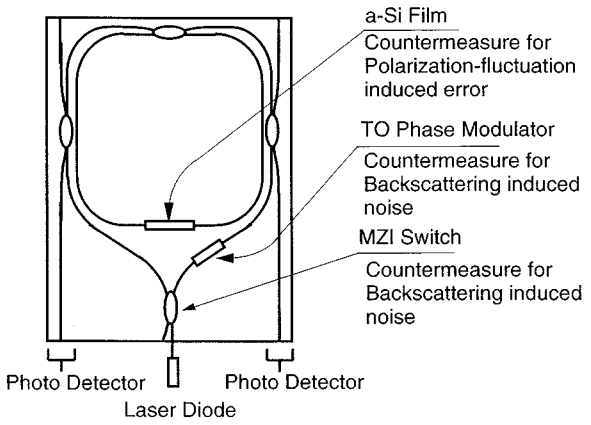

Fig. 1. Proposed configuration of resonator MOG on silica PLC with countermeasures for noise factors.

L resonator length.

Gyro sensitivity is maximized when the slope of the resonance dip becomes the largest. This is realized under the condition of

$$\gamma = \frac{2-3\kappa}{(2-\kappa)\sqrt{1-\kappa}}. \tag{3}$$

Namely, there is optimum κ for the loss of the waveguide.

Theoretical limitation of the rotation sensitivity in optical passive ring resonator gyro (OPRG) is determined by shot noise limit of the detector [13]. Fig. 2 represents the shot noise limit of the MOG, which is calculated under the optimization of (3). We can obtain the resolution of about the earth rotation rate even with 2 cm-diameter and one turn ring resonator as a sensing loop, as shown in Fig. 2. Here, we use typical parameters of PLC and other devices. Loss of waveguide and coupler are assumed to be 0.01 and 0.2 dB/cm, wavelength and linewidth of a light source 1.55 μm and 1 MHz, quantum efficiency of and optical power at photodiode 80% and 1 mW, bandwidth of gyro signal 1 Hz, respectively.

Micromachined gyroscopes may also achieve the same performance as the resonator microoptic gyro [14]. While they utilize the Coriolis effect, the optical gyros use the Sagnac effect. They may be smaller and cheaper than optical ones. However, it might be pointed out whether they have mechanical moving part or not. The microoptic gyro, as a gyro without any moving part, should be studied.

Resonance curve of fabricated PLC ring resonator is shown in Fig. 3. Fig. 3 is obtained with frequency tunable DFB-LD whose linewidth is 1 MHz. The parameters of this resonator is shown in Table I, which is obtained by fitting (1) to Fig. 3. Solid line and dashed line in Fig. 3 gives measured resonance curve and fitted curve, respectively. A directional coupler, which launches lightwave into the resonator, is composed of a Mach–Zehnder interferometer with a thermooptic phase shifter. Then, the coupling ratio is variable by the phase shifter, while the loss of it is relatively higher than a simple directional coupler. Considering the optimization of (3) and the parameters of the resonator listed in Table I, the shot noise limit of the fabricated resonator gyro is calculated as 2.9×10^{-3}°/s.

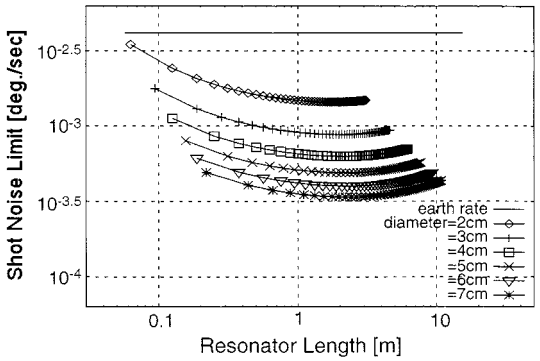

Fig. 2. Shot noise limit of the resonator PLC MOG.

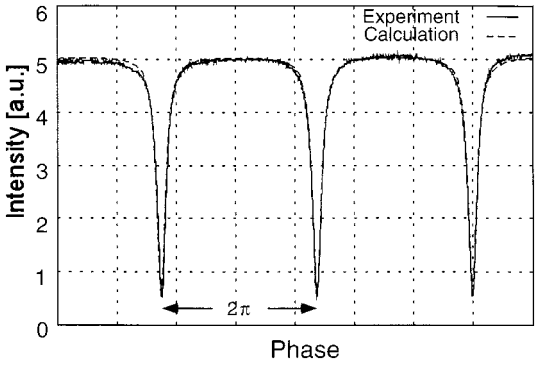

Fig. 3. Resonance curve of fabricated PLC ring resonator under selective excitation of one ESOP.

TABLE I
PARAMETERS IN FABRICATED PLC RESONATOR

resonator length	14.8cm
coupling ratio of directional coupler	variable
waveguide transmissivity γ_w	0.921
waveguide loss	0.024dB/cm
directional coupler transmissivity γ_c	0.949
directional coupler loss	0.23dB
Free Spectral Range	1.39GHz

C. Noise Factors in Optical Passive Ring-Resonator Gyro

Generally, OPRG's suffer from several noise factors listed in Table II, which also shows countermeasures for them.

In the sensing loop, two eigenstates of polarization (ESOP's) exist except for special case, and one ESOP is usually orthogonal to the other. The shapes of the ESOP's are changed due to the environmental fluctuations and they move independently with each other. This makes noise in the gyro output. In resonator fiber-optic gyro (R-FOG), polarization axis of polarization maintaining fiber is rotated by 90° at spliced point to suppress this polarization fluctuation induced noise [15]. In this case, two resonance dips corresponding to the two ESOP's are fixed and their separation is equals to π in phase.

However, in PLC's, it is difficult to rotate the polarization axis by 90°. Of course, it is possible to insert a half wave plate in the resonator [16]. However the loss of the resonator becomes

TABLE II
NOISE FACTORS AND COUNTERMEASURES FOR THEM IN OPRG's

Noise Factor	Countermeasure for Resonator Fiber Optic Gyro (R-FOG)	Proposed Countermeasure for Resonator Micro Optic Gyro (MOG)
Polarization fluctuation induced noise	Splicing the PM fiber with 90° polarization axis tilt	Tuning the waveguide birefringence with stress applying film
Backscattering induced noise	Suppression of carrier with b-PSK (binary Phase Shift Keying)	Combination of b-PSK, optical switch, and electrical gating
Kerr effect induced noise	Controlling CW and CCW lightwave power to be equal	No influence

higher, and the sensitivity of the gyro becomes lower. Therfore, we have proposed a method to use stress applying amorphous silicon film to control the birefringence of the waveguide as a practical countermeasure [17]. Laser trimming of amorphous silicon film has been developed to control the birefringence of the waveguide [17]. This can be used to make the two resonance dips of the ring resonator separated as π. This way makes a sense because the PLC resonator is quite stable compared with the fiber resonator. More discussion will be done in Section III.

Backscattering induced noise is the most serious noise factor in OPRG, for whom binary phase shift keying (B-PSK) is effective as countermeasure. Takiguchi and Hotate showed the performance of B-PSK in the resonator fiber-optic gyro with acoustooptic modulator [18]. Lightwave modulated with B-PSK does not have its carrier signal. Then, interference of the backscattered lightwave and the counter propagating signal lightwave is put out of the gyro bandwidth. However, we have only thermooptic phase modulator to apply the B-PSK in the PLC, whose bandwidth is limited just to 1 KHz in silica waveguide. Therefore, we think out a novel signal processing method which effectively utilizes the narrow bandwidth of the TO phase modulator. Detail will be discussed in Section IV.

III. COUNTERMEASURE FOR POLARIZATION FLUCTUATION INDUCED NOISE

A. Eigenstate of Polarization in Waveguide Ring-Resonator

Polarization fluctuation induced noise originates from the change of the birefringence in the waveguide. The conditions to have the resonance are

1) phase shift of a round-trip through the resonator equals to 2π and
2) state of polarization must be the same at any point in the resonator after one round-trip.

The polarization state which satisfies these conditions is called eigenstate of polarization (ESOP) and two orthogonal ESOP's exist simultaneously except special case [15]. Two eigenvectors of Jones matrix of one round trip through the resonator represent the two ESOP's and the eigenvalues give resonance frequencies of the resonator. These two resonance dips move independently, and one resonance modifies the shape of the other. This is the mechanism of the polarization fluctuation induced noise.

Ring resonator on a PLC usually suffers unavoidable small coupling between transverse electric (TE) and transverse magnetic (TM) mode, and birefringence in the waveguide. Jones matrix of the birefringent waveguide is expressed as

$$\boldsymbol{T} = \begin{pmatrix} e^{j\Delta\beta L} & 0 \\ 0 & e^{-j\Delta\beta L} \end{pmatrix} \tag{4}$$

and that of unavoidable coupling between TE and TM mode is given as

$$\boldsymbol{R} = \begin{pmatrix} \cos\theta & \sin\theta \\ -\sin\theta & \cos\theta \end{pmatrix} \tag{5}$$

where

β propagation constant;
L resonator length;
θ coupling angle of TE and TM mode, respectively.

Whole propagation matrix of the resonator is the product of (4) and (5). The eigenvalues are given by

$$\lambda = \cos\theta \cdot \cos(\Delta\beta L) \pm j\sqrt{1 - \cos^2\theta \cdot \cos^2(\Delta\beta L)} \tag{6}$$

and the eigenvectors are calculated as

$$\boldsymbol{u}_1 = \begin{pmatrix} j\left\{\cos\theta \cdot \sin(\Delta\beta L) + \sqrt{1 - \cos^2\theta \cdot \cos^2(\Delta\beta L)}\right\} \\ -\sin\theta \cdot e^{j\Delta\beta L} \end{pmatrix} \tag{7}$$

$$\boldsymbol{u}_2 = \begin{pmatrix} \sin\theta \cdot e^{j\Delta\beta L} \\ j\left\{\cos\theta \cdot \sin(\Delta\beta L) + \sqrt{1 - \cos^2\theta \cdot \cos^2(\Delta\beta L)}\right\} \end{pmatrix}. \tag{8}$$

As phase difference between TE and TM mode changes, the ESOP's change their shape. If $\Delta\beta L \approx 0$, the two eigenvalues are almost the same, and eigenvector gives counter rotating circular polarizations. In this case, it is impossible to distinguish two ESOP's with each other, and then the polarization noise will appear because the two resonance dips are excited equally. On the other hand, when $\Delta\beta L = \pi$ satisfied, resonance dips are fixed at the point separated as π from each other. Additionally, the two ESOP's have the shape of the linear polarizations being orthogonal with each other, under the condition of $\theta \approx 0$. The polarization directions of the ESOP's coincides with the polarization axes of the birefringent waveguide. Consequently, we

propose a way to eliminate the crossing of the two resonance dips:

1) to fix one resonance dip at the center of the other resonance interval (i.e., two ESOP's are set symmetrically) by controlling the waveguide birefringence;
2) to excite one polarization mode of the waveguide.

When $\Delta\beta L = \pi$, the two ESOP's are set to the condition 1. This situation is achieved by putting the stress applying amorphous silicon film on the waveguide and trimming it with laser [17]. Additionally, we must excite only one polarization mode of the waveguide (condition 2).

B. Experimental Result

As discussed above, it is possible to eliminate the polarization fluctuation induced noise when $\Delta\beta L = \pi$. This condition is realized with the stress applying amorphous silicon film. Laser trimming of a-Si film changes pressure applied to the waveguide, and adjusts the propagation constant of TE and TM mode [17]. This is the practical countermeasure. However, in the experiments shown below, we control the waveguide temperature instead of utilizing the stress applying amorphous silicon film. Heating the waveguide has the same effect as sticking the amorphous silicon film, so we can simulate the proposed method.

Fig. 4(a) shows the resonance curve under the worse condition of $\Delta\beta L \approx 0$, and Fig. 4(b) represents that under $\Delta\beta L = \pi$. In Fig. 4(b), both TE and TM mode are excited to clarify the relative position of ESOP's. Only TE or TM mode must be excited to suppress the polarization fluctuation induced noise when the system works as gyro. Fig. 3 was measured under such a condition.

Fig. 4(a) and (b) is measured by using a different PLC ring resonator from that in Fig. 3, according to experimental convenience. The thermal coefficient of the birefringence of the device in Fig. 4(a) and (b) is larger than that in Fig. 3. Namely, in the ring resonator shown in Fig. 3, relative position of the two ESOP's changes by π as the temperature of the waveguide varies about 60°C. This means that once the optimum ESOP is fixed by trimming of amorphous silicon film, the resonator has a tolerance, at least, as several tens of degrees Celsius.

IV. Countermeasure for Backscattering Induced Noise

A. Backscattering-Noise Reduction using Binary Phase Shift Keying with Novel Signal Processing Method

Backscattering induced noise originates from the Rayleigh backscattering or the Fresnel reflections inside and outside of the ring resonator. PLC's have relatively high loss and some fabrication defects [19], so the backscattering induced noise affects the MOG more severely than the R-FOG.

The signal E_s and the undesirable backscattered light E_b arrive at a photodiode, then the power at the photodiode is expressed as

$$I = |E_s|^2 + |E_b|^2 + 2\mathrm{Re}[E_s E_b^*] \tag{9}$$

where $*$ means complex conjugate. In (9), the first term represents the signal, the second one, the power of backscattered and/or reflected lightwave, and the last, the interference of the signal and the backscattered lightwave. Fluctuation of the interference term due to the phase variation of the backscattered light makes a dominant noise in the gyro output. Backscattered light intensity $|E_b|^2$ does not make the random noise, though it induces nonlinearity in the gyro output [13]. Then, the interference term must be suppressed at least. The countermeasure is schematically shown in Fig. 1. Suppression of the interference noise is achieved by the TO phase modulator arranged at an arm, which is driven by B-PSK modulation. To reduce the influence of the backscattered light intensity, the time division switching should addtionally be done between the counter propagating lightwaves by the Mach–Zehnder interferometric switch.

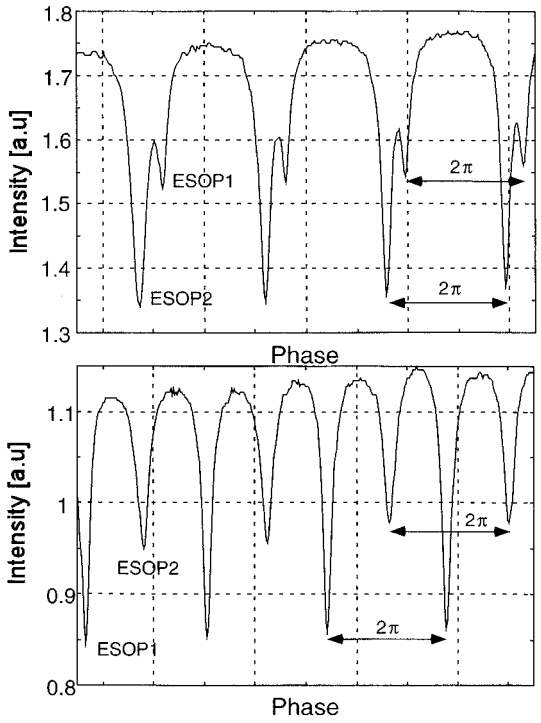

Fig. 4. Resonance curve: (a) under $\Delta\beta L \simeq 0$ and (b) under $\Delta\beta L \simeq \pi$.

The signal lightwave and the backscattered lightwave is given by

$$E_s(t) = E_0 e^{j\{\omega t + \phi(t)\}} \tag{10}$$

$$E_b(t) = R E_0 e^{j\{\omega t + \xi\}} \tag{11}$$

respectively, where

E_0 amplitude of the input light;
ω optical angular frequency;
ξ ensemble averaged phase of the backscattered light;
$\phi(t)$ phase change in the TO phase modulator;
R equivalent reflection ratio, respectively.

Then, one can get the interference term as

$$2\,\mathrm{Re}[E_s E_b^*] = 2RE_0^2\,\cos\{\xi + \phi(t)\}. \tag{12}$$

B-PSK is the method to modulate the lightwave as

$$\phi(t) = \begin{cases} 0 \\ \pi \end{cases} \tag{13}$$

through the TO phase modulator. So far, in R-FOG, B-PSK is considered as a method to eliminate the carrier signal, and then the interference is pushed out of gyro bandwidth. However, we had found that the average between 0 phase and π phase makes the interference turn to be zero. The bandwidth of the TO phase modulator is limited just to 1 KHz. To utilize the narrow bandwidth of the TO phase modulator fully, we adopt the signal series shown in Fig. 5. A and B in Fig. 5 represents lasing frequencies of the light source, which is modulated in frequency shift keying, in order to track the resonance frequency of the resonator. The optical switch alternates the direction of the lightwave to the laser modulation in twice the speed. In each term, the lightwave is modulated as 0 and π, and average between 0 phase and π phase makes the true value of the signal without the influence of the interference term, which are represented by the dashed lines. Then, the difference of the signals with the same suffix makes the tracking signal for the laser frequency and the gyro output, respectively. Namely, $A^R - B^R$ is for the feedback control of the laser frequency, and $A^L - B^L$ is for the gyro output. Electrical gating is introduced to hide the transient part of the phase and the intensity modulation. Consequently, we can get the same signal rate as the LD modulation frequency.

B. Experimental Result

Dominant noise source is the interference term, so we apply only the B-PSK as the countermeasure in the experiment.

To track a resonance dip by changing the light source frequency with a high accuracy, feedback speed must be as high as possible. As mentioned above, however, the possible feedback speed is limited by the bandwidth of the TO phase modulator. Moreover, the square shape in the phase modulation waveform gets broken, as the modulation speed becomes higher. Here we try to expand the bandwidth of the TO phase modulator by using a frequency compensating modulation signal.

By using the gyro setup, the response of the TO modulator with the ordinary square modulation waveform is measured. Fig. 6 shows the experimental setup to measure the response. The results are shown in Fig. 7. From Fig. 7(a), the time constant of the TO phase modulator is measured as 1.57 ms. There exists time delay of 0.22 ms in our thermo-optic phase modulator.

Due to the response of the TO modulator, the flat region in the output of the MZI is quite narrow. To expand the flat region, we propose a compensating modulation waveform, which is designed considering the time constant obtained above. The shape is shown in Fig. 7(b). It is clear, from Fig. 7(b), that the interferometer output is flattened by this waveform with overshoot. The highest modulation speed of 400 Hz is obtained for the TO phase modulator. This is limited, at this time, by the ability of the electronic devices such as analog-to-digital (A/D) to digital-to-analog (D/A) converters or microcomputer.

With the countermeasures described above, the gyro output noise is measured. The results shown in Fig. 8(a)–(c) gives the gyro output with no countermeasure, the square modulation waveform, and the designed overshoot modulation waveform, respectively. The time constant is 1.57 ms. The phase modulation waveforms are shown also in Fig. 8(b) and (c). The gyro output with the ordinary square modulation waveform and that with the compensating modulation waveform has a noise level of about 100 and 40°/s, respectively. They are 3.9 and 7.6 dB down compared to the case without the countermeasures.

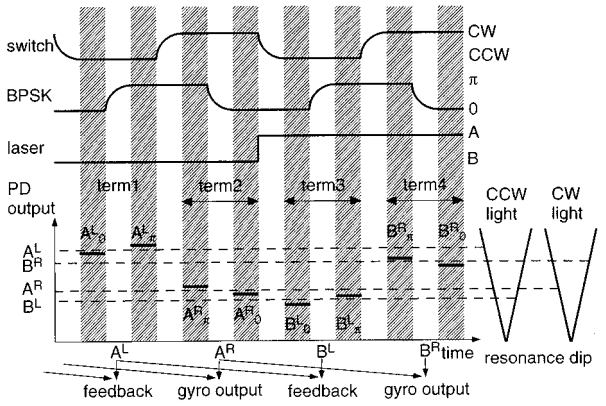

Fig. 5. Schematic diagram of proposed signal processing with narrow bandwidth of TO modulators.

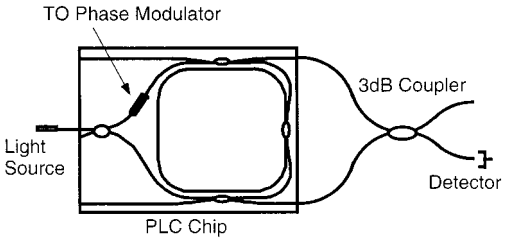

Fig. 6. Experimental setup for measuring time constant of the TO phase modulator.

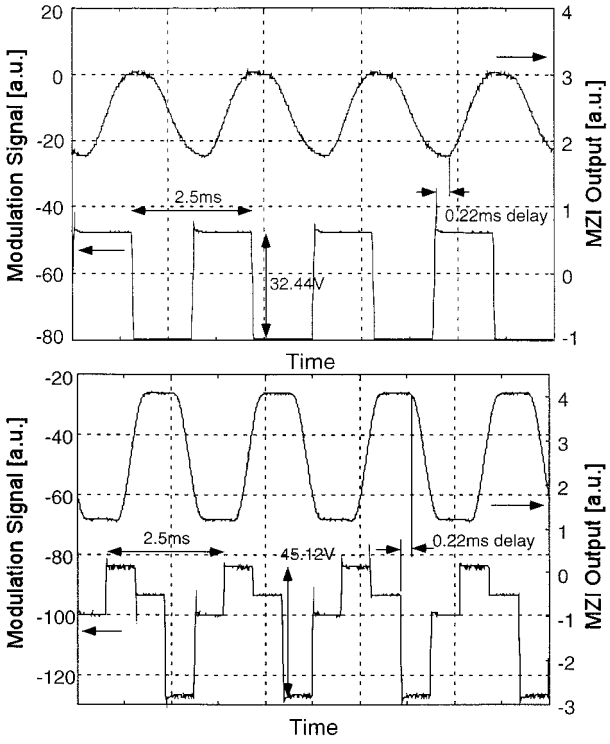

Fig. 7. Modulation signal waveform and interferometer output: (a) with ordinary square phase modulation and (b) with designed overshoot phase modulation.

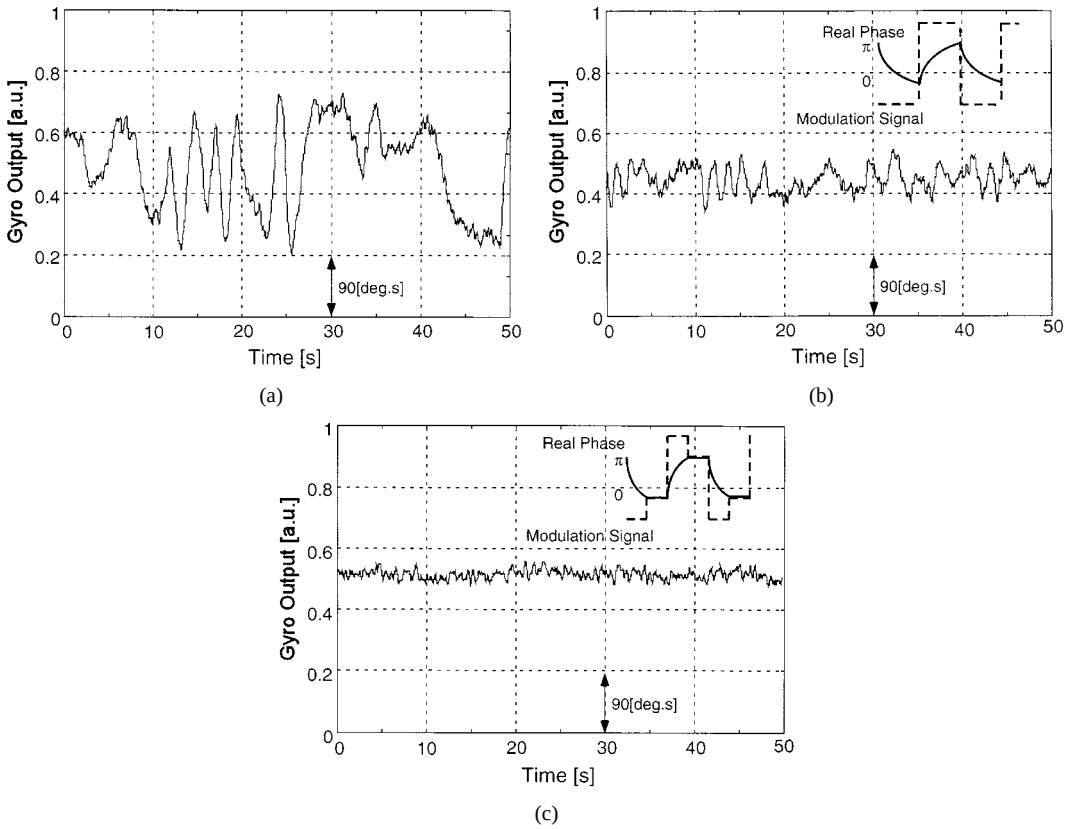

Fig. 8. Gyro output: (a) Without countermeasure for the backscattering induced noise, (b) with ordinary square phase modulation for B-PSK, and (c) with designed overshoot phase modulation for B-PSK. Integration time: 0.4 s.

Fig. 9 shows the degradation of the noise suppression due to the amplitude error in the B-PSK modulation. Deviation from the ideal amplitude of π, degrades the noise suppression ratio. In this calculation, it is supposed that the bandwidth of the modulator is infinite. The noise suppression ratio of 7.6 dB corresponds to the error of around 10% in modulation amplitude, which is larger than expected. The reason of the unsatisfactory suppression ratio might be that the B-PSK frequency is not high enough compared with that of the phase fluctuation of the backscattered lightwave in the present system with fiber pig-tailed devices. Another reason is the frequency chirp in the LD. The frequency chirp brings the gradual change in the phase of the lightwave, which makes the initial phase ξ of the interference term in (12) not to be constant. Accordingly, the interference term in 0 and π phase in Fig. 5 does not show the same absolute value with the opposite sign. This results in the offset in the gyro output. Flattening of the FM response of the LD can solve this problem.

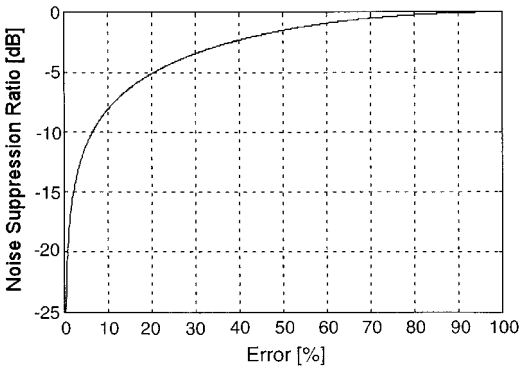

Fig. 9. Degradation of the backscattering induced-noise suppresion due to the error in the B-PSK amplitude.

V. Rotation Sensing

With the countermeasures for the polarization fluctuation induced noise and the backscattering induced noise, we measured the gyro output. For the experimental convenience, we applied equivalent rotation by giving electrical offset to the feedback loop, instead of actual rotation. Because the noise level is still large, it is required to apply a rather high rotation rate. On the other hand, we have external components in the experimental setup, such as the LD and the PD's connected to PLC via optical fibers. Then it is hard for us to rotate the system actually. Fig. 10 shows the result of the rotation measurement. The input rotation rate is 120°/s, and the time constant of the gyro output is 400 ms.

VI. Conclusion

In this paper, we have proposed a novel configuration of the resonator microoptic gyro on the silica planar lightwave circuit with the countermeasures for noise factors. These countermeasures are for the polarization fluctuation induced noise and the backscattering induced noise. The former noise is reduced by adjusting the separation between the two ESOP's with control of the waveguide birefringence. The suppression of the latter

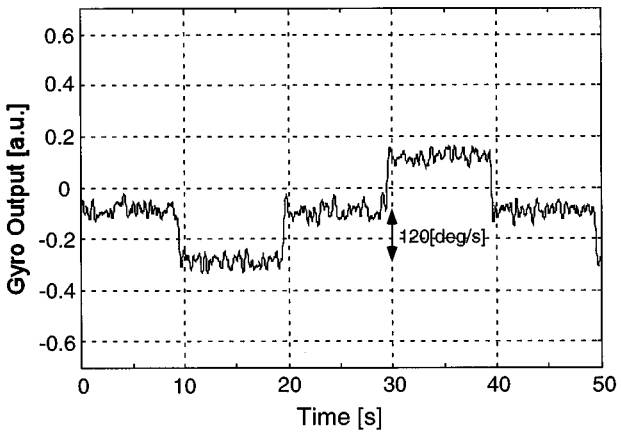

Fig. 10. Rotation measurement with quasirotation input. Integration time: 0.4 s.

noise is achieved by B-PSK modulation with the waveform designed for compensating the frequency response of the TO modulator in the PLC and the electronic gating. We have shown the effectiveness of the countermeasures in the experiment. The rotation measurement has demonstrated, applying equivalent rotation, by the setup with the countermeasures.

REFERENCES

[1] H. C. Lefèvre, *The Fiber-Optic Gyroscope*. Norwood, MA: Artech House, 1993.
[2] K. Hotate, "Fiber-optic gyros," in *Optical Fiber Sensors*, J. Dakin and B. Culshow, Eds. Norwood, MA: Artech House, 1997, vol. II, pp. 167–206.
[3] ——, "Fiber sensor technology today," *Optic. Fiber Technol.*, vol. 3, pp. 356–401, 1997.
[4] K. Iwatsuki, M. Saruwatari, M. Kawachi, and H. Yamazaki, "Waveguide-type optical passive ring-resonator gyro using time division detection scheme," *Inst. Elect. Eng. Electron. Lett.*, vol. 25, no. 11, pp. 689–688, 1989.
[5] A. Lawrence, "Providing an inexpensive gyro for the navigation mass market," in *Proc. Inst. Navigation Nat. Tech. Meeting*, San Diego, CA, 1990, pp. 161–166.
[6] P. Mottier and P. Pouteau, "Solid state optical gyrometer integrated on silicon," *Inst. Elect. Eng. Electron. Lett.*, vol. 33, no. 23, pp. 1975–1977, 1997.
[7] D. Jestel, A. Baus, and E. Voges, "Integrated-optic interferometric microdisplacement sensor in glass with thermo-optic phase modulation," *Electron. Lett.*, vol. 26, no. 15, pp. 1144–1145, 1990.
[8] O. G. Helleso, P. Benech, and R. Rimet, "Displacement sensor made by potassium diffusion on glass," *J. Lightwave Technol.*, vol. 12, pp. 568–572, Mar. 1994.
[9] M. Ohkawa, M. Izutsu, and T. Sueta, "Integrated optic pressure sensor on silicon substrate," *Appl. Opt.*, vol. 25, no. 23, pp. 5153–5157, 1989.
[10] T. Storgaard-Larsen, S. Bouwstra, and O. Leistiko, "Opto-mechanical accelerometer based on strain sensing by a Bragg grating in a planar waveguide," *Sens. Actuators A*, vol. 52, pp. 25–32, 1996.
[11] V. Minier, D. Persegol, J. L. Lovato, and A. Kevorkian, "Integrated optical current sensor for high-power systems," in *Proc. OFS-11*, Sapporo, Japan, 1996, We2-3, pp. 164–167.
[12] S. Ezekiel and S. R. Balsamo, "Passice ring resonator laser gyroscope," *Appl. Phys. Lett.*, vol. 30, no. 9, pp. 478–480, 1977.
[13] K. Iwatsuki, K. Hotate, and M. Higashiguchi, "Effect of Rayleigh backscattering in an optical passive ring-resonator gyro," *Appl. Opt.*, vol. 23, no. 21, pp. 3916–3924, 1984.
[14] N. Yazdi, F. Ayazi, and K. Najafi, "Micromachined inertial sensor," *Proc. IEEE*, vol. 86, no. 8, pp. 1640–1659, 1998.
[15] K. Hotate, "Polarization problem and countermeasures in passive/active resonator fiber optic gyros *(Invited Paper)*," *Proc. SPIE*, vol. 2292, pp. 227–239, 1994.
[16] Y. Inoue, A. Kaneko, F. Hanawa, H. Takahashi, K. Hattori, and S. Sumida, "Athermal silica-based arrayed-waveguide grating multiplexer," *Inst. Elect. Eng. Electron. Lett.*, vol. 33, no. 23, pp. 1945–1947, 1997.
[17] M. Okuno, A. Sugita, K. Jinguji, and M. Kawachi, "Birefringence control of silica waveguide on Si and its application to polarization beam splitter/switch," *J. Lightwave Technol.*, vol. 12, pp. 625–633, 1994.
[18] K. Hotate, K. Takiguchi, and A. Hirose, "Adjustment-free method to eliminate the noise induced by the backscattering in an optical passive ring-resonator gyro," *IEEE Photon. Technol. Lett.*, vol. 2, pp. 75–77, Jan. 1990.
[19] K. Takada, H. Yamada, Y. Hida, Y. Ohmori, and S. Mitachi, "Rayleigh backscattering measurement of 10 m long silica-based waveguides," *Inst. Elect. Eng. Electron. Lett.*, vol. 32, no. 18, pp. 1665–1667, 1996.

Kenya Suzuki was born in Sapporo, Japan, in 1971. He received the B.E. and the M.E. degrees in electrical engineering, from the University of Tokyo, Tokyo, Japan, in 1995 and 1997, respectively. He is now working toward the Dr.Eng. degree at the same university.

His current research interest is in integrated microoptic gyroscopes.

Mr. Suzuki is a student member of the Institute of Electronics, Information and Communication Engineers (IEICE) of Japan.

Koichi Takiguchi (M'92) was born in Ibaraki Prefecture, Japan. He received the B.S. degree in electronics engineering and the M.S. and Ph.D. degrees in electrical engineering, all from the University of Tokyo, Tokyo, Japan, in 1987, 1989, and 1992, respectively. His dissertation was in resonator-type fiber-optic gyro (RFOG).

In 1992, he joined NTT Laboratories, Japan, where he was engaged in research on silica-based planar waveguide devices and high-speed optical transmission systems. He is now interested in optical signal processing devices and its application to next generation optical communication systems and networks at NTT Photonics Laboratories, Ibaraki Prefecture. From 1998 to 1999, he worked as a Visiting Scholar at the University of California, Santa Barbara (UCSB), investigating modulation characteristics of long-wavelength vertical-cavity lasers.

Dr. Takiguchi is a member of the Institute of Electronics, Information and Communication Engineers (IEICE) of Japan, and Optical Society of Japan (OSJ).

Kazuo Hotate (M'91–SM'98) was born in Tokyo, Japan, on June 20, 1951. He received B.E., M.E., and Dr.Eng. degrees in electronics engineering, all from the University of Tokyo, Tokyo, Japan, in 1974, 1976 and 1979, respectively.

In 1979, he joined the University of Tokyo as a Lecturer. He became Associate Professor in 1987, and Professor in 1993 in the Research Center for Advanced Science and Technology (RCAST), the University of Tokyo. Since 1997, he has been Professor in Department of Electronic Engineering, School of Engineering, The University of Tokyo. He was engaged in research of projection-type holography, and measurement and analysis of optical fiber characteristics. At present, he is working on optoelectronics-applied measurement and optical computing. He is a coauthor of the books *Optical Fibers* (Tokyo, Japan: Ohm-Sha, 1982, in Japanese) and *Optical Fiber Sensors* (Tokyo, Japan: Ohm-Sha, 1986, in Japanese).

Dr. Hotate received the Achievement Award in 1979 and the Book Award in 1984 both from the Institute of Electronics, Information and Communication Engineers (IEICE) of Japan, the Paper Award on "Optical Fiber Gyro" in 1984 from the Society of Instrument and Control Engineers of Japan (SICE), and the Best Papers Award of the forth Optoelectronics Conference in 1992. He is a member of IEICE, SICE, the Institute of Electrical Engineers of Japan, the Institute of Television Engineers of Japan, the Optical Society of Japan, and the Japan Society for Aeronautical and Space Sciences.